Laser-induced breakdown of the magnetic-field-reversal symmetry in the propagation of unpolarized light

G. S. Agarwal and Shubhrangshu Dasgupta
Physical Research Laboratory, Navrangpura, Ahmedabad-380 009, India
(Received 12 June 2002; published 28 February 2003)

We show how a medium, under the influence of a coherent control field that is resonant or close to resonance to an appropriate atomic transition, can lead to very strong asymmetries in the propagation of unpolarized light when the direction of the magnetic field is reversed. We show how electromagnetically induced transparency (EIT) can be used in atomic vapor to mimic this magnetochiral effect that occurs in natural systems. EIT can produce much larger asymmetry than the well-known magnetochiral effect as we use the dipole-allowed transitions here. Using density-matrix calculations we present results for the breakdown of the magnetic-field-reversal symmetry for two different atomic configurations.

DOI: 10.1103/PhysRevA.67.023814 PACS number(s): 42.50.Gy, 78.20.Ls, 33.55.−b

I. INTRODUCTION

It is well known how an isotropic medium becomes anisotropic by the application of a magnetic field [1]. In the special case when the magnetic field is parallel to the direction of the applied field and if we include the electric dipole contribution to susceptibilities, then the two circularly polarized light waves travel independently of each other. The propagation itself is determined by the magnetic-field-dependent optical susceptibilities $\chi_{\pm}$. If we write the incident field of frequency ω in the form

$$\vec{E} \equiv (\mathcal{E}_{+}\hat{\epsilon}_{+} + \mathcal{E}_{-}\hat{\epsilon}_{-})e^{ikz-i\omega t} + \text{c.c.}, \tag{1}$$

where

$$\hat{\epsilon}_{\pm} = \left(\frac{\hat{x} \pm i\hat{y}}{\sqrt{2}}\right), \quad \mathcal{E}_{\pm} = \left(\frac{\mathcal{E}_x \mp i\mathcal{E}_y}{\sqrt{2}}\right), \quad k = \frac{\omega}{c}, \tag{2}$$

the output field is given by

$$\vec{E}_0 = \vec{\mathcal{E}}_0 e^{ikz-i\omega t} + \text{c.c.}, \tag{3}$$

where

$$\vec{\mathcal{E}}_0 = \mathcal{E}_{+}\hat{\epsilon}_{+}e^{2\pi ikl\chi_{+}} + \mathcal{E}_{-}\hat{\epsilon}_{-}e^{2\pi ikl\chi_{-}}. \tag{4}$$

The susceptibilities $\chi_{\pm}$ also depend on the frequency of the applied field. The rotation of the plane of polarization [2–7] and the dichroism can be calculated in terms of the real and imaginary parts of $\chi_{\pm}$. An interesting situation arises if the incident pulse is unpolarized. In that case there is a random phase difference between $\mathcal{E}_x$ and $\mathcal{E}_y$ and the intensities along two orthogonal directions are equal, i.e.,

$$\langle \mathcal{E}_x^* \mathcal{E}_x \rangle = \langle \mathcal{E}_y^* \mathcal{E}_y \rangle = \frac{I}{2}, \qquad \langle \mathcal{E}_x^* \mathcal{E}_y \rangle = 0, \tag{5}$$

I being the intensity of the incident pulse. From Eqs. (2)–(5), we can evaluate the output intensity $I_0 = \langle |\vec{\mathcal{E}}_0|^2 \rangle$,

$$\begin{aligned} I_0 &\equiv \frac{I}{2}[|e^{2\pi ikl\chi_{+}}|^2 + |e^{2\pi ikl\chi_{-}}|^2] \\ &= \frac{I}{2}[\exp\{-4\pi kl\,\text{Im}(\chi_{+})\} + \exp\{-4\pi kl\,\text{Im}(\chi_{-})\}]. \end{aligned} \tag{6}$$

Thus the output intensity is a symmetric function of χ_{+} and χ_{-}. If the susceptibilities $\chi_{\pm}$ obey the following relation when the direction of the magnetic field is reversed:

$$\chi_{\pm}(B) = \chi_{\mp}(-B), \tag{7}$$

then

$$I_0(B) = I_0(-B). \tag{8}$$

Thus for unpolarized light the output intensity is the same whether the magnetic field is parallel or antiparallel to the direction of propagation of the electromagnetic field, as long as Eq. (7) is satisfied.

In this paper we investigate if the transmission of unpolarized light through an otherwise isotropic medium can be sensitive to the direction of the magnetic field. We demonstrate how a suitably applied control field could make the transmission dependent on the direction of the magnetic field. This is perhaps the first demonstration of the dependence of transmission of the unpolarized light on the direction of B in an atomic vapor. For a large range of parameters we find that transmission could be changed by a factor of order 2. We also report a parameter domain where the medium becomes opaque for one direction, but becomes transparent for the reversed direction of the magnetic field. This work is motivated by the phenomena of optical activity and the magnetochiral anisotropy which occur in many systems in nature [8–10]. The latter effect has recently become quite important. Several ingenious measurements of this effect have been made, though the effect in natural systems is quite small. The smallness of the effect arises from the fact that the effect involves a combination of electric dipole, magnetic dipole, and quadrupole effects [11–14]. The magnetochiral anisotropy is just the statement $I(B)$ not equal to $I(-B)$. The effect we report is analogous but quite different in its physical content as the one reported here arises from electric dipole transitions unlike the traditional one that arises from higher-order multipole transitions.

In this paper we show how rather large asymmetry between $I_0(B)$ and $I_0(-B)$ can be produced by using a coherent control field. The asymmetry could be large as we use only the electric dipole transitions. To demonstrate the idea we consider different specific situations depending on the transition on which the control field is applied. The control field can be used to modify, say, χ_+ leaving χ_- unchanged [2,4,6,15]. Thus in presence of the control field we violate the equality (7) and this can result in large magneto-asymmetry in the propagation of unpolarized light. Such a large asymmetry, which we would refer to as magnetic-field-reversal asymmetry (MFRA in short), is induced by selectively applying the control field so as to break the time-reversal symmetry. It is important to note that we work with electric dipole transitions only and this is the reason we distinguish it from the effect arising from a term in polarization which is a product of B and k. The control field is used to mimic the effects that occur in nature due to a combination of higher-order multipole transitions.

The structure of our paper is as follows. In Sec. II, we will discuss how one can use a control field to create large MFRA. We present a very simple physical model. We present relevant analytical results. In Sec. III, we introduce another model, where the control field is applied such that we get a ladder system. We present the analytical results for MFRA in such a system. We also discuss the effect of atomic motion on MFRA in Sec. IV.

II. LARGE MAGNETIC-FIELD-REVERSAL ASYMMETRY USING EIT

The application of a coherent pump leads to the well-studied electromagnetically induced transparency (EIT) [15] and coherent population trapping [16]. The usage of pump and probe in a Λ configuration is especially useful in suppressing the absorption of the probe, particularly if the lower levels of the Λ configuration are metastable and if the pump is applied between initially unoccupied levels. We explore how EIT can help in producing large MFRA. We first explain the basic idea in qualitative terms and then would produce detailed results using density-matrix equations for several systems of interest.

Consider the following scenario. Let us consider first the case when $\vec{B}$ is applied parallel to the direction of propagation of the electromagnetic field. Suppose the control field is applied such that the σ_+ component becomes transparent, i.e., $\mathrm{Im}[\chi_+(B)]\approx 0$. For magnetic field bigger than the typical linewidth, the component σ_- is off resonant. Thus σ_- exhibits very little absorption $\mathrm{Im}(\chi_-)\approx 0$. Under such conditions, Eq. (6) shows that the transmitted intensity $\approx I$. Now if the direction of the magnetic field is reversed, then we easily find the situation when σ_+ component becomes off resonant from the corresponding transition, i.e., $\mathrm{Im}(\chi_+)\approx 0$; the σ_- component can become resonant and suffers large absorption, i.e., exhibits large $\mathrm{Im}(\chi_-)$. This gives rise to an intensity $\sim I/2$. Thus the transmittivity reduces by a factor 1/2 upon reversal of the magnetic field. It is thus clear how coherent fields can be used to create large MFRA.

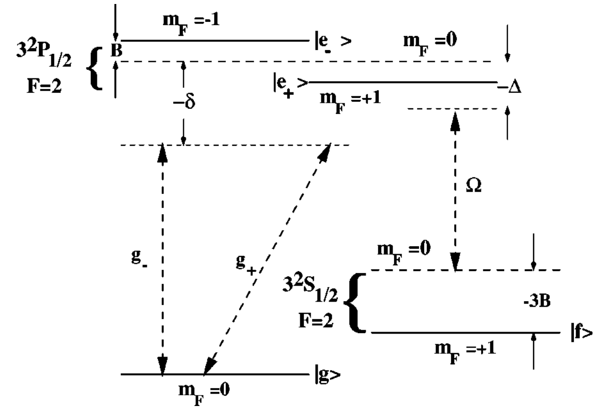

FIG. 1. The ^{23}Na hyperfine level configuration is shown here. Here, $B>0$ is the applied magnetic-field strength, $2g_\pm$ are the probe Rabi frequencies for the $\sigma_\pm$ components, and Ω is the half of the pump Rabi frequency. The respective detunings $\delta=[\omega_p-\omega_{e_+g}(B=0)]$ and Δ for the probe and pump fields are defined with respect to the energy separation between the levels $(|3^2P_{1/2};F=2,m_F=0\rangle,|g\rangle)$ and $(|3^2P_{1/2};F=2,m_F=0\rangle,|3^2S_{1/2};F=2,m_F=0\rangle)$, respectively. Changing the direction of the magnetic field interchanges the positions of $|e_-\rangle$ and $|e_+\rangle$. Besides, the level $|f\rangle$ moves above the dashed line for $|3^2S_{1/2};F=2,m_F=0\rangle$.

We now demonstrate the feasibility of these ideas. We consider a configuration (see Fig. 1) that can be found, for example, in hyperfine levels of ^{23}Na [17]. The level $|g\rangle$ $(|3^2S_{1/2};F=1,m_F=0\rangle)$ is coupled to the upper levels $|e_-\rangle$ $(|3^2P_{1/2};F=2,m_F=-1\rangle)$ and $|e_+\rangle$ $(|3^2P_{1/2};F=2,m_F=+1\rangle)$ by the σ_- and σ_+ components of the probe field, respectively. The susceptibilities for the two components of the probe acting on the transitions $|g\rangle\leftrightarrow|e_-\rangle$ and $|g\rangle\leftrightarrow|e_+\rangle$ are given by

$$\chi_-(B)=\frac{-i\gamma\alpha_0}{i(\delta-B)-\Gamma_{e_-g}}, \tag{9a}$$

$$\chi_+(B)=\frac{-i\gamma\alpha_0}{i(\delta+B)-\Gamma_{e_+g}}, \quad \delta\equiv\omega-\omega_{e_+g}(B=0), \tag{9b}$$

where α_0 is given by $N|\vec{d}|^2/\hbar\gamma$ and is related to the absorption in the line center for $B=0$. It should be borne in mind that B represents the Zeeman splitting of the level $m_F=-1$. Thus B has the unit of frequency. Here 2γ is the spontaneous decay rate from the level $|e_-\rangle$, $\Gamma_{e_-g}=\gamma(\Gamma_{e_+g}=4\gamma/3)$ is the decay rate of the off-diagonal density-matrix elements between levels $|e_-\rangle$ $(|e_+\rangle)$ and $|g\rangle$, N is the atomic number density, $|\vec{d}|$ is the dipole moment matrix element between the levels $|e_-\rangle$ and $|g\rangle$, and δ is the detuning of the probe field from the $|g\rangle\leftrightarrow|3^2P_{1/2};F=2,m_F=0\rangle$ transition. Note that δ would always be defined with respect to the levels in the absence of the magnetic field. Using Eqs. (6) and (9), one easily finds that the relation (8) holds for all δ. In all equations, B would be considered as a positive quantity.

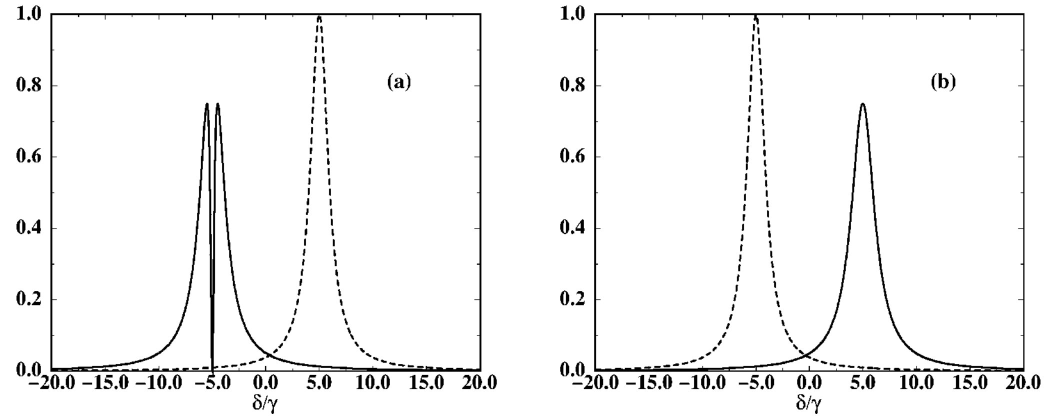

FIG. 2. The variation of imaginary parts of the susceptibilities $\overline{\chi_+}$ (solid curve) and $\overline{\chi_-}$ (dashed curve) in units of α_0 with probe detuning δ/γ are shown for $\overline{\chi_\pm}(B)$ (a) and $\overline{\chi_\pm}(-B)$ (b). The parameters used here are $\Omega=0.5\gamma$, $B=5\gamma$ corresponding to 105 G, $\Gamma_{e_+g}=4\gamma/3$, $\Gamma_{fg}=0$, $\Gamma_{e_-g}=\gamma$, and $\Delta=2B$.

To create a large asymmetry between the output intensities $I_0(B)$ and $I_0(-B)$, we now apply a coherent control field

$$\vec{E}_p(z,t)=\vec{\mathcal{E}}_p(z)e^{-i\omega_p t}+\text{c.c.} \tag{10}$$

on the transition $|e_+\rangle \leftrightarrow |f\rangle$ ($|3^2S_{1/2};F=2,m_F=+1\rangle$). This modifies the susceptibility χ_+ of the σ_+ component to

$$\overline{\chi_+}(B)=\frac{-i\gamma\alpha_0[i(\delta-\Delta+3B)-\Gamma_{fg}]}{[i(\delta+B)-\Gamma_{e_+g}][i(\delta-\Delta+3B)-\Gamma_{fg}]+|\Omega|^2},$$

$$\Delta=\omega_p-\omega_{e_+f}(B=0). \tag{11}$$

Here, $\Delta=2B$ is the detuning of the pump field from the transition $|3^2P_{1/2};F=2,m_F=0\rangle \leftrightarrow |3^2S_{1/2};F=2,m_F=0\rangle$ transition (see Fig. 1), $\Omega=\vec{d}_{e_+f}\cdot\vec{\mathcal{E}}_p/\hbar$ is the half of the pump Rabi frequency. The parameter Γ_{fg} represents the collisional dephasing between the states $|f\rangle$ and $|g\rangle$. In what follows we use $\Gamma_{fg}=0$. The level $|f\rangle$ is Zeeman separated from the level $|3^2S_{1/2};F=2,m_F=0\rangle$ by an amount of $3B$, whereas the levels $|e_\pm\rangle$ are separated by an amount $\mp B$. These can be calculated from the Landé-g factor of the corresponding levels. The susceptibility $\overline{\chi_-}$ remains the same as in Eq. (9a). Note that in the presence of the control field, the response of the system is equivalent to a two-level system comprising ($|e_-\rangle,|g\rangle$) (for the σ_- component) and a Λ system (for the σ_+ component) comprising ($|e_+\rangle,|f\rangle,|g\rangle$) connected via the common level $|g\rangle$.

It is clear that applying a coherent pump field, one can generate an EIT window at $\delta=-B$ (cf. $\Delta=2B$) for the σ_+ component [Im $(\overline{\chi_+})=0$]. On the other hand, the absorption peak of the σ_- component occurs at $\delta=B$. Thus, this component suffers a little absorption [Im $(\overline{\chi_-})\approx 0$] at $\delta=-B$ as the field is far detuned from the $|e_-\rangle \leftrightarrow |g\rangle$ transition as long as we choose the magnetic field much larger than the width of the transition [see Fig. 2(a)]. Thus, the unpolarized probe field travels through the medium almost unattenuated. The transmittivity $T(B)=I_0(B)/I$ becomes almost unity at $\delta=-B$ as obvious from Eq. (6) (see Fig. 3).

If now the direction of the magnetic field is reversed ($B\rightarrow -B$), then the corresponding susceptibilities for σ_- and σ_+ polarizations become

$$\overline{\chi_-}(-B)=\frac{-i\gamma\alpha_0}{i(\delta+B)-\Gamma_{e_-g}}, \tag{12a}$$

$$\overline{\chi_+}(-B)=\frac{-i\gamma\alpha_0[i(\delta-\Delta-3B)-\Gamma_{fg}]}{[i(\delta-B)-\Gamma_{e_+g}][i(\delta-\Delta-3B)-\Gamma_{fg}]+|\Omega|^2}. \tag{12b}$$

We continue to take the quantization axis as defined by the direction of propagation of the electromagnetic field. Clearly now at $\delta=-B$, $\overline{\chi_-}(-B)$ has an absorption peak and the σ_- component of the probe will be absorbed. If we continue to use $\Delta=2B$, i.e., if we keep the control laser frequencies fixed while we change the direction of the magnetic field,

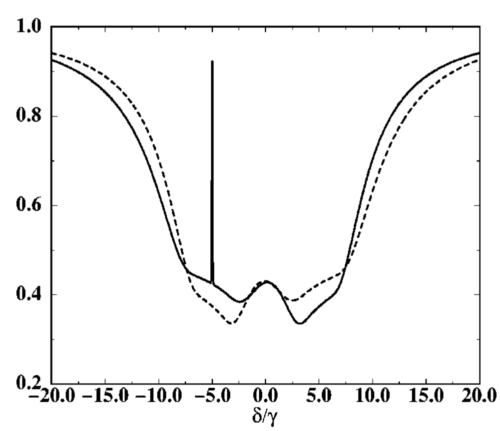

FIG. 3. This figure shows the variation of the transmittivities $T(B)$ (solid curve) and $T(-B)$ (dashed curve) with respect to probe field detuning δ/γ. The parameters used here are $N=10^{10}$ atoms cm^{-3}, $\lambda=589$ nm, and $L=1$ cm. All the other parameters used are the same as in Fig. 2.

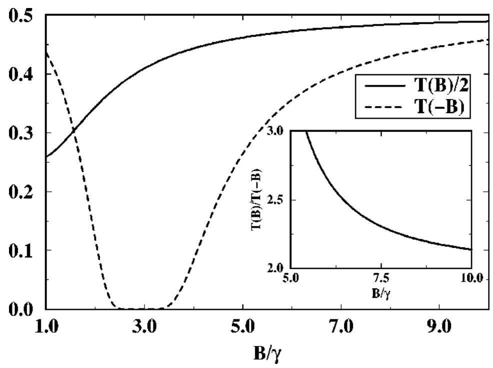

FIG. 4. The transmittivities $T(B)$ and $T(-B)$ calculated at the value $\delta=-B$ are plotted here with respect to B/γ, for $\Omega=10\gamma$ and $\Delta=2B$. The inset shows the magnetic-field dependence of the ratio $T(B)/T(-B)$ for the same parameters. All the other parameters are the same as in Fig. 3.

then $\overline{\chi}_{+}(-B)$ exhibits resonances at $\delta=3B\pm\sqrt{4B^2+\Omega^2}$, both of which are far away from the point $\delta=-B$ unless we choose $\Omega^2=12B^2$. Clearly, for $\delta=-B$ and $\Omega^2\neq 12B^2$, the σ_+ component of the probe will suffer very little absorption. This is in contrast to the behavior of the σ_- component, which will be attenuated by the medium. Thus the output field would essentially have the contribution from the σ_+ component. The transmittivity $T(-B)=I_0(-B)/I$ of the medium decreases to about 1/2. Thus by using EIT we can produce the result $T(B)\approx 2T(-B)$, i.e., we can alter the transmittivity of the medium by just reversing the direction of the magnetic field. The equality (8) is no longer valid and the medium behaves like a chiral medium. This becomes quite clear from Fig. 3, at $\delta=-B$.

A quite different result is obtained by choosing the parameter region differently. For the choice of the external field strength $\Omega=2\sqrt{3}B$, and $\Delta=2B$, $\delta=-B$, the σ_+ component gets absorbed significantly if the direction of the magnetic field is opposite to the direction of propagation of the field. Thus $T(-B)$ becomes insignificant compared to $T(B)$, as shown in Fig. 4. For larger values of B, the result is shown in the inset. Here $T(B)/T(-B)$ is in the range 2 to 3. Clearly, the case displayed in Fig. 4 is quite an unusual one. Such a large asymmetry in the dichroism of unpolarized light is the result of the application of a coherent control field whose parameters are chosen suitably.

The behavior shown in Fig. 4 is easily understood from the magnitudes of the imaginary parts of the susceptibilities $\overline{\chi}_{\pm}(\pm B)$. In the parameter domain under consideration, $\mathrm{Im}[\overline{\chi}_{+}(B)]=0$ (EIT); $\mathrm{Im}[\overline{\chi}_{-}(-B)]=\alpha_0$, because the σ_- component is on resonance for $\vec{B}$ antiparallel to the direction of propagation. Further, as shown in the Fig. 5, in the region around $\Omega=2\sqrt{3}B$, $\mathrm{Im}[\overline{\chi}_{-}(B)]\ll\mathrm{Im}[\overline{\chi}_{+}(-B)]$. Thus, both σ_- and σ_+ components are absorbed if $\vec{B}$ is antiparallel to $\vec{k}$, making the medium opaque as shown in the inset of Fig. 5. The opacity disappears if direction of $\vec{B}$ is reversed (see Fig. 4, solid curve). For values of B away from the equality $\Omega=2\sqrt{3}B$, $\mathrm{Im}[\overline{\chi}_{+}(-B)]$ decreases leading to an increase in the transmission $T(-B)$.

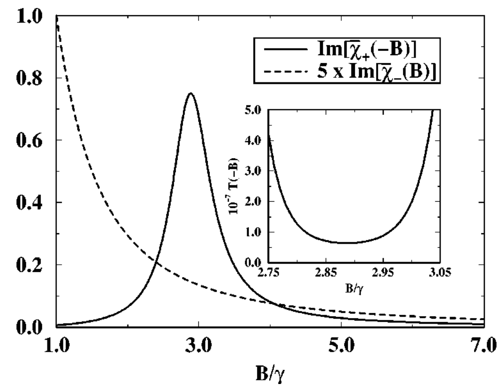

FIG. 5. The variation of the imaginary parts of the susceptibilities $\overline{\chi}_{+}(-B)$ and $\overline{\chi}_{-}(B)$ in units of α_0 with the magnetic field B/γ for $\delta=-B$. The inset shows the variation $T(-B)$ with B in the vicinity of $\Omega=2\sqrt{3}B$. The parameters used here are the same as in Fig. 4.

We conclude this section by examining the symmetry properties of the Hamiltonian under the transformation $B\to -B$. We note from Fig. 1 that the unperturbed Hamiltonian in the absence of the control field is

$$H_0=(-\delta-B)|e_+\rangle\langle e_+|+(-\delta+B)|e_-\rangle\langle e_-|. \quad (13)$$

A transformation $B\to -B$ is like interchanging the states $|e_+\rangle$ and $|e_-\rangle$. Thus any physical result that involves states $|e_\pm\rangle$ symmetrically will not change by changing the direction of $\vec{B}$. This is the case with the transmission (6). Next, when we apply the control field Ω, then the unperturbed Hamiltonian is

$$H_0=(-\delta-B)|e_+\rangle\langle e_+|+(-\delta+B)|e_-\rangle\langle e_-|+(-\delta+\Delta-3B)|f\rangle\langle f|+\Omega(|e_+\rangle\langle f|+|f\rangle\langle e_+|). \quad (14)$$

The states $|e_+\rangle$ and $|f\rangle$ are mixed by the control field with an amount of mixing that is dependent on the magnetic field. Clearly we have lost the symmetry property of H_0 and hence of the transmission (6). It is easily seen that Eq. (13) has the time-reversal symmetry whereas Eq. (14) has no such symmetry.

III. LARGE MAGNETIC-FIELD-REVERSAL ASYMMETRY IN A LADDER SYSTEM

It may be recalled that there are many different situations where a pump cannot be applied in a Λ configuration. This, say, for example, is the case for ^{40}Ca. The relevant level configuration is shown in Fig. 6 [4]. The level $|g\rangle$ ($|4s^2;j=0,m_j=0\rangle$) is coupled to $|e_+\rangle$ ($|4s4p;j=1,m_j=+1\rangle$) and $|e_-\rangle$ ($|4s4p;j=1,m_j=-1\rangle$) via the σ_+ and σ_- components of the input unpolarized probe field, respectively. In this configuration, the susceptibilities of the two circularly polarized components of the probe are given by

$$\chi_+(B)=\frac{-i\gamma\alpha_0}{i(\delta-B)-\gamma}, \quad (15a)$$

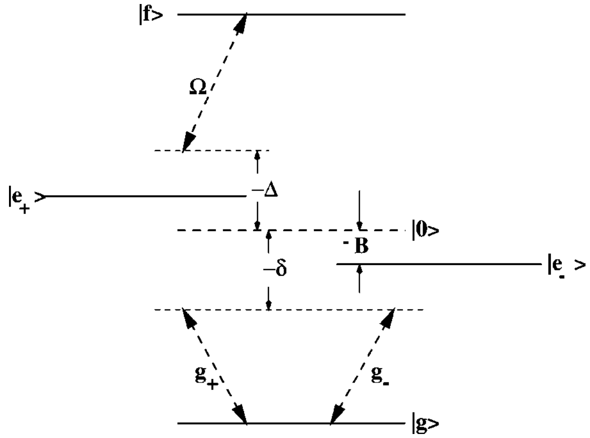

FIG. 6. The ^{40}Ca level configuration has been shown here. Here, $2g_{\pm}$ are the probe Rabi frequencies for the $\sigma_{\pm}$ components, B is the magnetic-field strength, Ω is the half of the pump Rabi frequency, δ and Δ are the respective detunings for the probe and the pump fields. These detunings are defined with respect to the energy separation between the levels $(|0\rangle,|g\rangle)$ and $(|0\rangle,|f\rangle)$, respectively.

$$\chi_{-}(B)=\frac{-i\gamma\alpha_0}{i(\delta+B)-\gamma},\quad \delta=\omega-\omega_{e_{-}g}(B=0), \quad (15b)$$

where $\alpha_0=N|\vec{d}|^2/\hbar\gamma$, N is the number density of the medium, δ is the detuning of the probe field with respect to the $|g\rangle\leftrightarrow|0\rangle$ $(|4s4p;j=1,m_j=0\rangle)$ transition, $|\vec{d}|$ is the magnitude of the dipole moment matrix element between the levels $|e_+\rangle$ and $|g\rangle$, and 2γ is the decay rate from the levels $|e_+\rangle$ and $|e_-\rangle$ to the level $|g\rangle$. Note that the imaginary parts of the susceptibilities (15) are peaked at $\delta=B$ and $\delta=-B$, respectively, and clearly predict perfect symmetry in the transmittivity of the medium upon reversal of the direction of the magnetic field.

We will now show how one can use a coherent control field to create asymmetry between $T(B)$ and $T(-B)$. We apply a coherent pump (10) to couple $|e_+\rangle$ with a higher excited level $|f\rangle$ $(|4p^2;j=0,m_j=0\rangle)$ with Rabi frequency

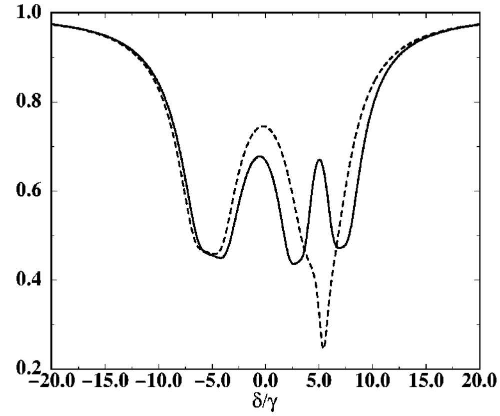

FIG. 8. The variation of the transmittivities $T(B)$ (solid curve) and $T(-B)$ (dashed curve) with the probe detuning δ/γ is shown in this figure. The parameters used here are $N=10^{10}$ atoms cm^{-3}, $\lambda_{e_+g}=422.7$ nm, $L=1$ cm, and the other parameters are the same as in Fig. 7.

$2\Omega=2\vec{d}_{fe_+}\cdot\vec{\mathcal{E}}_p/\hbar$. The susceptibility for σ_+ component now changes to [2]

$$\overline{\chi_{+}}(B)=\frac{-i\gamma\alpha_0[i(\Delta+\delta)-\Gamma]}{[i(\delta-B)-\gamma][i(\Delta+\delta)-\Gamma]+|\Omega|^2},$$

$$\Delta=\omega_p-\omega_{fe_+}(B=0), \quad (16)$$

where $\Gamma=0.5(\lambda_{e_+g}/\lambda_{fe_+})^3\gamma=0.45\gamma$ is the spontaneous decay rate of the upper level $|f\rangle$ [cf. $\lambda_{e_+g}=422.7$ nm and $\lambda_{fe_+}=551.3$ nm], $\lambda_{\alpha\beta}$ is the wavelength of the transition between $|\alpha\rangle$ and $|\beta\rangle$, $\Delta=-B$ is the detuning of the pump field from the $|f\rangle\leftrightarrow|0\rangle$ transition (see Fig. 6). Thus a transparency dip in the absorption profile of the σ_+ component at $\delta=B$ is generated and the σ_- component remains far detuned from the corresponding transition, as shown in Fig. 7(a). Note that the transparency for σ_+ is not total, which is in contrast to a Λ system. We display in Fig. 8 the behavior

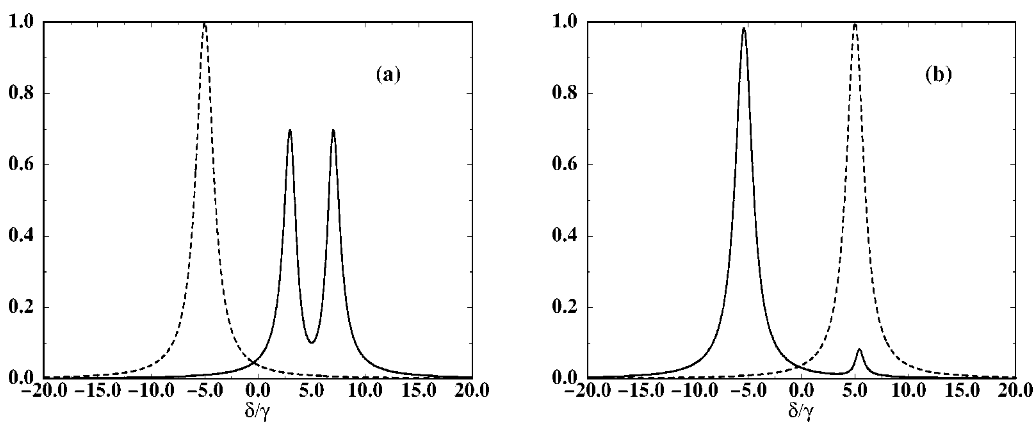

FIG. 7. The variation of imaginary parts of the susceptibilities $\overline{\chi_+}$ (solid curve) and $\overline{\chi_-}$ (dashed curve) in units of α_0 with respect to the probe detuning δ/γ is shown here for $\overline{\chi_\pm}(B)$ (a) and $\overline{\chi_\pm}(-B)$ (b). The parameters used here are $\Omega=0.5\gamma$, $B=5\gamma$ corresponding to 123 G, $\Gamma=0.45\gamma$, and $\Delta=-B$.

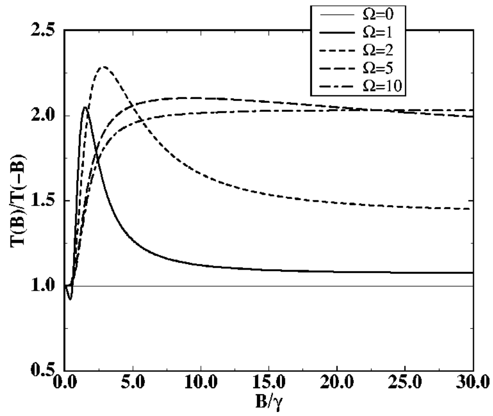

FIG. 9. The variation of the ratio $T(B)/T(-B)$ calculated at $\delta = B$ with the magnetic-field strengths B/γ is shown in this figure for different values of Ω. All the parameters are the same as in Fig. 8.

of the transmittivity $T(B)$ of the medium as a function of the detuning.

Now upon reversal of the magnetic-field direction, the σ_+ component gets detuned from corresponding transition and thereby suffers little absorption. The σ_- component, being resonant with the corresponding transition, gets largely attenuated inside the medium. This is clear from Fig. 7(b). Thus the contribution to the transmittivity $T(-B)$ comes primarily from the σ_+ component. Figure 8 exhibits the behavior of $T(-B)$ as the frequency of the probe is changed. In the region of EIT, $T(B)$ is several times of $T(-B)$.

In Fig. 9, we have shown how the ratio $T(B)/T(-B)$ calculated at $\delta=B$ is modified with change in the magnitude of the applied magnetic field for different control field Rabi frequencies. Note that for large B and Ω, this ratio approaches the value of 2, though for intermediate values it can exceed 2.

IV. MAGNETIC-FIELD-REVERSAL ASYMMETRY IN THE PROPAGATION OF AN UNPOLARIZED BEAM THROUGH A DOPPLER BROADENED MEDIUM

We next consider the effects of Doppler broadening on the MFRA in a Λ configuration. We would like to find parameter regions where $T(B)$ and $T(-B)$ could differ significantly. We identify the spatial dependence of the pump $\mathcal{E}_p(z) = e^{ik_p z}$ and $\Delta_v = 2B + k_p v_z$, where v_z is the component of the atomic velocity in the direction of propagation of the electric fields. We assume that the pump field propagates in the same direction $\vec{k}_p$ as the probe field wave vector $\vec{k}$ and we further take k and k_p to be approximately equal.

We calculate the Doppler-averaged susceptibilities through the following relation:

$$\langle \overline{\chi}_\pm(v_z) \rangle = \int_{-\infty}^{\infty} \overline{\chi}_\pm(v_z)\sigma_D(v_z)dv_z, \tag{17}$$

where

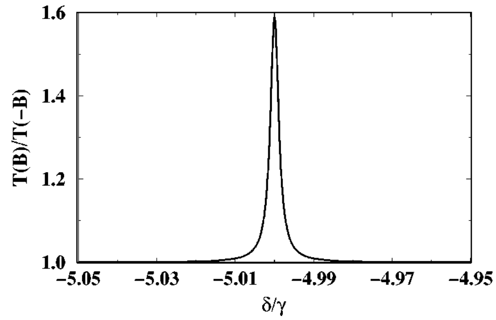

FIG. 10. The variation in $T(B)/T(-B)$ with the probe detuning δ/γ in a 6-cm Doppler-broadened medium. All the other parameters are the same as in Fig. 4. Note that $T(B)$ is the transmission for $\vec{B}$ parallel to $\vec{k}$.

$$\sigma_D(v_z) = \frac{1}{\sqrt{2\pi\omega_D^2}} e^{-v_z^2/2\omega_D^2} \tag{18}$$

is the Maxwell-Boltzmann velocity distribution at a temperature T with the width $\omega_D = \sqrt{k_B t/M}$, k_b is the Boltzmann constant, and M is the mass of an atom.

The integration (17) results in a complex error function [18]. However, to have a physical understanding, we integrate Eq. (17) by approximating σ_D by a Lorentzian $\sigma_L(v_z)$ of the width $\tilde{\omega}_D = 2\omega_D \ln 2$ [19],

$$\sigma_L(v_z) = \frac{\tilde{\omega}_D/\pi}{v_z^2 + \tilde{\omega}_D^2}. \tag{19}$$

This leads to the following approximate results:

$$\langle \overline{\chi}_\pm(v_z) \rangle = \frac{\gamma\alpha_0}{k(v_\pm - i\tilde{\omega}_D)}, \tag{20}$$

where

$$v_+ = \frac{i\{[i(\delta+B) - \Gamma_{e_+g}]P + |\Omega|^2\}}{kP},$$

$$P = i(\delta - \Delta + 3B) - \Gamma_{fg},$$

$$v_- = \frac{i[i(\delta-B) - \Gamma_{e_-g}]}{k}. \tag{21}$$

Here we have used expressions (9a) and (11) for $\overline{\chi}_\pm(v_z)$. These susceptibilities (20) are used to calculate the transmittivities at the point $\delta = -B$. In Fig. 10 we have shown the corresponding variation of $T(B)$ and $T(-B)$ with δ/γ. We find that the ratio $T(B)/T(-B)$ increases to a value ~ 1.6 for a 6-cm medium. It is clear that if we choose a longer medium in this case, the MFRA will be further enhanced. We have actually also carried out numerically the integration (17). For the parameters of Fig. 10, the results do not change substantially.

V. CONCLUSIONS

In conclusion, we have shown how one can make use of a coherent field to create large MFRA in the propagation of an unpolarized light beam. We have discussed two different system configurations. We have shown how EIT can be used very successfully to produce large MFRA. We have also analyzed the effect of Doppler broadening and found the interesting region of parameters with large asymmetry.

[1] L.D. Landau, E.M. Lifshitz, and L.P. Pitaevski, *Electrodynamics of Continuous Media* (Pergamon, Oxford, 1984).

[2] A.K. Patnaik and G.S. Agarwal, Opt. Commun. **179**, 97 (2000).

[3] M.O. Scully and M. Fleischhauer, Phys. Rev. Lett. **69**, 1360 (1992); M. Fleischhauer and M.O. Scully, Phys. Rev. A **49**, 1973 (1994); M. Fleischhauer, A.B. Matsko, and M.O. Scully, *ibid.* **62**, 013808 (2000).

[4] S. Wielandy and A.L. Gaeta, Phys. Rev. Lett. **81**, 3359 (1998).

[5] B. Stahlberg, P. Jungner, T. Fellman, K.-A. Suominen, and S. Stenholm, Opt. Commun. **77**, 147 (1990); K.-A. Suominen, S. Stenholm, and B. Stahlberg, J. Opt. Soc. Am. B **8**, 1899 (1991).

[6] A.K. Patnaik and G.S. Agarwal, Opt. Commun. **199**, 109 (2001); V.A. Sautenkov, M.D. Lukin, C.J. Bednar, I. Novikova, E. Mikhailov, M. Fleischhauer, V.L. Velichansky, G.R. Welch, and M.O. Scully, Phys. Rev. A **62**, 023810 (2000).

[7] D. Budker, V. Yashchuk, and M. Zolotorev, Phys. Rev. Lett. **81**, 5788 (1998); D. Budker, D.F. Kimball, S.M. Rochester, V.V. Yashchuk, and M. Zolotorev, Phys. Rev. A **62**, 043403 (2000).

[8] G.L.J.A. Rikken and E. Raupach, Phys. Rev. E **58**, 5081 (1998).

[9] G.L.J.A. Rikken and E. Raupach, Nature (London) **390**, 493 (1997).

[10] M. Vallet, R. Ghosh, A. Le Floch, T. Ruchon, F. Bretenaker, and J.-Y. Thépot, Phys. Rev. Lett. **87**, 183003 (2001).

[11] G. Wagnière and A. Meier, Chem. Phys. Lett. **93**, 78 (1982).

[12] L.D. Barron and J. Vrbancich, Mol. Phys. **51**, 715 (1984).

[13] N.B. Baranova and B.Ya. Zel'dovich, Mol. Phys. **38**, 1085 (1979).

[14] L.D. Barron, Nature (London) **405**, 895 (2000).

[15] S.E. Harris, Phys. Today **50**(7), 46 (1997).

[16] E. Arimondo, in *Progress in Optics XXXV*, edited by E. Wolf (Elsevier, New York, 1996), p. 257.

[17] I. Carusotto, M. Artoni, G.C. La Rocca, and F. Bassani, Phys. Rev. Lett. **87**, 064801 (2001).

[18] M. Abramowitz and I.A. Stegun, *Handbook of Mathematical Functions* (Dover, New York, 1972).

[19] M.M. Kash, V.A. Sautenkov, A.S. Zibrov, L. Hollberg, G.R. Welch, M.D. Lukin, T. Rostovtsev, E.S. Fry, and M.O. Scully, Phys. Rev. Lett. **82**, 5229 (1999).